

Muon-spin-rotation measurements in the *kagomé* lattice systems: Cr-jarosite and Fe-jarosite

A. Keren,* K. Kojima, L. P. Le,† G. M. Luke, W. D. Wu, and Y. J. Uemura
Department of Physics, Columbia University, New York, New York 10027

M. Takano
Institute for Chemical Research, Kyoto University, Uji, Kyoto-fu 611, Japan

H. Dabkowska
Department of Physics and Astronomy, McMaster University, Hamilton, Ontario, Canada L8S 4M1

M. J. P. Gingras
TRIUMF, 4004 Wesbrook Mall, Vancouver, British Columbia, Canada V6T 2A3
 (Received 15 September 1995)

We have examined the magnetic properties of the frustrated *kagomé* lattice spin systems $\text{KFe}_3(\text{OH})_6(\text{SO}_4)_2$ (Fe-jarosite) and $\text{KCr}_3(\text{OH})_6(\text{SO}_4)_2$ (Cr-jarosite) using the μSR technique. In Fe-jarosite, a clear muon precession signal in zero field was found below 55 K, corresponding to the long-range order of Fe moments. In Cr-jarosite spin fluctuations persist without clear signature of spin freezing even at $T = 25$ mK, far below $T_g \sim 2$ K where the history dependence in the magnetic susceptibility appears.

Magnetic moments on the two-dimensional *kagomé* lattice, coupled with an antiferromagnetic (AFM) nearest-neighbor interaction, exhibit unusual magnetic behavior.¹⁻⁴ For example, numerical/theoretical works have shown that Ising spins on the *kagomé* lattice are known to be disordered down to zero temperature,⁵ while in the Heisenberg model there are excitations with finite amplitude even for infinitesimally small excitation energy.⁶ These phenomena result from the high degeneracy of the classical ground state, which could lead to strong dynamical spin fluctuations even at very low temperatures.

Most of the experimental effort in *kagomé* systems has concentrated on $\text{SrCr}_x\text{Ga}_{12-x}\text{O}_{19}[\text{SCGO}(x)]$.^{1,2,7,8} Indeed, unusual dynamical properties were reported by both neutron scattering and μSR .^{2,8} However, SCGO does not serve as a perfect realization of the AFM *kagomé* lattice,⁹ since non-magnetic Ga atoms partially substitute magnetic Cr sites in SCGO ($x < 9.0$) and since SCGO has alternating magnetic planes with *kagomé* and triangular lattices. Previous studies in SCGO were performed in $x \leq 8.0$. In this paper, we extend the μSR investigation to the family of compounds known as the jarosites, $\text{KFe}_3(\text{OH})_6(\text{SO}_4)_2$ (Fe-jarosite: Fe^{3+} , $S=5/2$), and $\text{KCr}_3(\text{OH})_6(\text{SO}_4)_2$ (Cr-jarosite: Cr^{3+} , $S=3/2$). These systems have a full stack of *kagomé* planes and involve, at least nominally, no randomness in ionic configuration,^{10,11} which is ideal for the experimental study of the *kagomé* lattice.

Fe-jarosite (Fe-JST) has been studied extensively by neutron-scattering, magnetic-susceptibility (χ), and Mössbauer measurements,^{11,12} which indicate that Fe moments undergo long-range magnetic order below $T_N \sim 50$ K, with the so-called $q=0$ type 120° spin structure. The ordered moment estimated by neutron and Mössbauer studies is about $4.3 \mu_B$, suggesting that the predominant component of the $S=5/2$ Fe moment becomes static at $T \rightarrow 0$. Extrapolation of the high-temperature susceptibility gives the Curie-Weiss

temperature (T_{cw}) ~ 600 K;^{11,12} indicating a large reduction of the energy scale for magnetic instability, $T_N/T_{\text{cw}}=0.08$, characteristic of geometrically frustrated spin systems.

Cr-jarosite (Cr-JST), on the other hand, has a Curie-Weiss temperature of 67.5 K,¹² while a departure of the field-cooled (FC) and zero-field-cooled (ZFC) susceptibility occurs only below $T_g \sim 2$ K as will be shown later. The ratio $T_g/T_{\text{cw}} \leq 0.03$ of this material indicates a suppression of magnetic instability temperature even more pronounced than in Fe-JST. A neutron-scattering measurement of Broholm *et al.*¹³ found a magnetic Bragg peak corresponding to the $q=0$ structure below $T = 1.9$ K. The intensity of this peak, however, was much weaker (about 1/10) than the expected value for the ordering of $S=3/2$ Cr moments; suggesting that either only a small volume fraction exhibits long-range order with $S=3/2$ or the entire volume participates in the magnetic order, but with a much reduced static spin component of $\sim 1 \mu_B$. In either case, one can expect strong dynamic spin fluctuations remaining at $T \rightarrow 0$.

We used powder samples of Fe-JST prepared at Kyoto University and Cr-JST prepared at McMaster University, following procedures described in Ref. 14. The μSR experiments were performed at TRIUMF, using a gas-flow cryostat for the Fe-JST measurements and an Oxford dilution refrigerator for the Cr-JST measurements. In order to obtain better cooling of the powder sample in the dilution refrigerator we mixed the powder with 10% Apiezon grease which was diluted in Hexane and allowed to dry for a day. This procedure did not change the susceptibility (per Cr) of the sample.

In a μSR experiment, a beam of 100% polarized muons is stopped, one by one, in a specimen. The muons come to rest within 10^{-10} sec, at a crystallographic site, with their polarization along the beam direction \hat{z} . Each spin then evolves in the local field until the μ^+ decays at a time t after its arrival. The decay positron is emitted preferentially along the muon-spin direction. Two counters placed forward (F) and back-

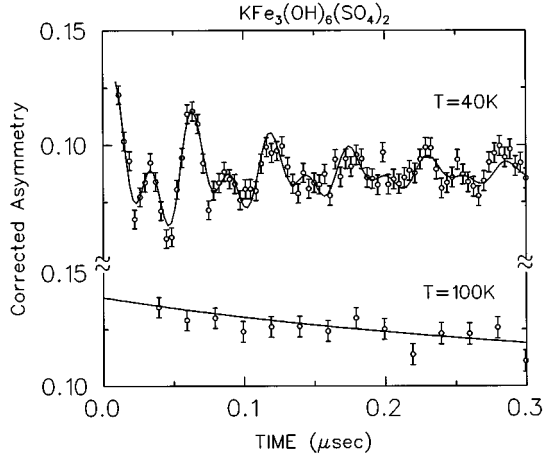


FIG. 1. The corrected asymmetry observed in $\text{KFe}_3(\text{OH})_6(\text{SO}_4)_2$ in zero external field.

ward (B) direction with respect to \hat{z} are used to obtain positron decay time histograms, which typically contain more than 10^6 events. From the $F(t)$ and $B(t)$ spectra, one derives the corrected asymmetry $A(t) = A_0 P_z(t)$, i.e., a product of the initial asymmetry $A_0 = 0.1 \sim 0.2$ (determined by the experimental configuration) and the muon spin polarization function $P_z(t)$.¹⁵

In Fig. 1 we show the observed corrected asymmetry measured in zero applied field. At 100 K the Fe moments fluctuate very rapidly and are ineffective in depolarizing the muon spin, but as the temperature is lowered these moments slow down. At lower temperatures ($T \leq 50$ K) full spin precession is seen. The inset of Fig. 2 shows the Fourier transform of the data at $T = 2.1$ K; two major frequencies are seen with a smaller contribution from a third signal which cannot be resolved in the fits. The frequencies at $T = 2.1$ K correspond to local fields of 2.8 and 1.6 kG, respectively, at the muon sites.

We fit the data below 45 K with a function assuming two frequencies

$$A(t) = A_b e^{-t/T_b} + \sum_{i=1}^2 A_i \exp(-t/T_1^{[i]}) \cos(2\pi \nu_i t), \quad (1)$$

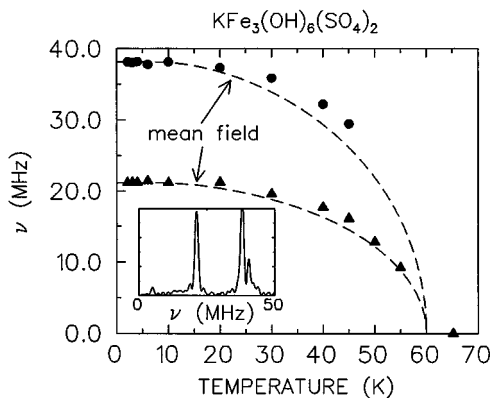


FIG. 2. The temperature dependence of the muon-spin precession frequency $\nu(T)$ in $\text{KFe}_3(\text{OH})_6(\text{SO}_4)_2$. The solid line represents the mean-field theory for spin 5/2. The inset shows the Fourier transform of corrected asymmetry at 2.1 K.

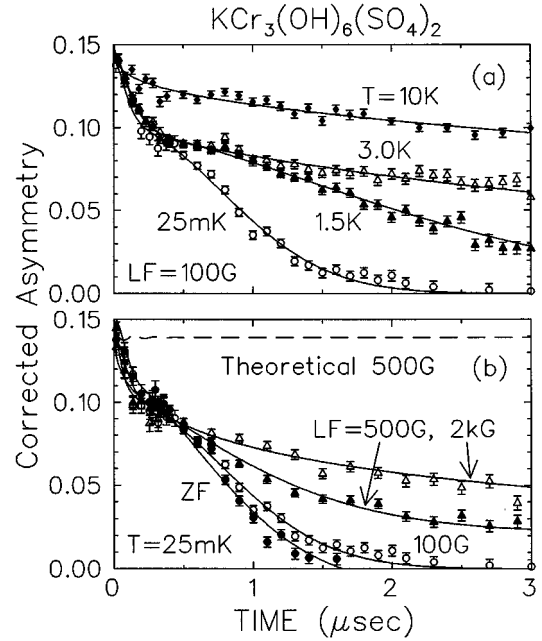


FIG. 3. The corrected asymmetry observed (a) in $\text{KCr}_3(\text{OH})_6(\text{SO}_4)_2$ in $H_L = 100$ G at several temperatures, and (b) in $\text{KCr}_3(\text{OH})_6(\text{SO}_4)_2$ at 25 mK in zero field and several longitudinal fields. The solid lines are guides to the eye. The broken line is the theoretical corrected asymmetry in $\text{LF} = 500$ G calculated for the case of relaxation due to static random field.

where the first term represents a background signal. The two frequencies can originate either from two crystallographically inequivalent muon sites or from a structurally unique but magnetically inequivalent site. Figure 2 presents the temperature dependence of the two frequencies, which represents the variation of staggered magnetization (local moment) in the system. (Above $T = 50$ K, we could not resolve the two frequencies.) For comparison we attach the mean-field theory curve for spin 5/2 assuming $T_N = 60$ K. The measured moment is more stable against thermal excitation than the mean-field prediction; this tendency was also found in previous Mössbauer measurements.¹²

The measurements in Cr-JST were performed in the longitudinal field (LF) configuration, where an external magnetic field H_L is applied along the beam direction \hat{z} . Figure 3(a) shows the corrected asymmetry observed in Cr-JST at several temperatures. Here a small longitudinal field of 100 G was applied to eliminate the effect of background signal and of the nuclear dipolar fields. The increase in relaxation as the system was cooled down from 10 K to 25 mK indicates the slowing down of spin fluctuations. Figure 3(b) shows the corrected asymmetry observed at $T = 25$ mK in zero-field and several different longitudinal applied fields. Even at the lowest temperatures well below T_g , no precession signal was observed in zero field, in a clear contrast to the case of Fe-JST shown in Fig. 1. At $T = 25$ mK, the results in zero field are essentially the same as that in $\text{LF} = 100$ G, except for slight differences which may be due to the effect of nuclear dipolar fields in the sample and also to possible systematic errors in estimating background for the zero-field measurements. Thus, we can assume that the weak LF ($\text{LF} = 100$ G) does not alter the essential features of $P_z(t)$.

Theories for the functional forms of $P_z(t)$ due to random local fields can be found in Refs. 16–18. In brief, important factors include the distribution of random fields (usually approximated by Gaussian in dense and Lorentzian in dilute spin systems), its width Δ/γ_μ (γ_μ is the gyromagnetic ratio of μ^+), the frequency ν of the dynamic fluctuations, and the external longitudinal field H_L . In static random fields ($\nu \ll \Delta$) with Gaussian (Lorentzian) distribution, $P_z(t)$ starts with Gaussian (exponential) decay at $t \rightarrow 0$. In zero field, the polarization recovers to $P_z(t) = 1/3$ at $t \rightarrow \infty$, since statistically 1/3 of the muons find their local field along the initial polarization direction z . As H_L increases, the local field (i.e., the vector sum of internal and external fields) is better aligned along z , and thus the asymptotic value $P_z(t \rightarrow \infty)$ increases. $P_z(t \rightarrow \infty) \sim 1$ for $\gamma_\mu H_L \geq 5\Delta$. This phenomenon is called “decoupling” by LF, and serves as a signature of relaxation due to static random fields.

In the fast dynamic case ($\nu/\Delta \geq 10$; narrowing limit) with Gaussian distribution, $P_z(t)$ is given by $\exp(-t/T_1)$ with $1/T_1 = 2\Delta^2\nu/(\omega_L^2 + \nu^2)$, without the 1/3 recovery. In an intermediate case with a moderate fluctuation rate $\nu \sim \Delta$, we still expect a Gaussian shape at early time $t \leq 1/\Delta$, with a substantial decoupling effect by H_L , but $P_z(t)$ keeps a slow decay afterwards. In Lorentzian random fields with dilute spins, a root-exponential decay $\exp[-(t/T_1)^{0.5}]$ is expected in the narrowing limit.

Several important features can be found in the observed results of Cr-JST in Fig. 3(b) at $T = 25$ mK: (i) There are two different signals with different relaxation rates superimposed. (ii) $P_z(t)$ in zero field shows monotonic decay without recovery to 1/3, suggesting involvement of a dynamic effect. (iii) The dependence on H_L is very weak. The broken line in Fig. 3(b) corresponds to the decoupling effect for $H_L = 500$ G expected if the observed relaxation were caused by static random local fields. The much smaller field dependence in the observed results suggests that, in both the slow and fast relaxing signals, the relaxation is due to dynamic fields in the regime of fast (but not intermediate) fluctuations. (iv) However, both of these two signals exhibit a Gaussian-like decay in early times.

To account for the results in Cr-JST quantitatively, we fit the corrected asymmetry $A(t)$ to the sum of two power-exponential functions

$$A(t) = \sum_{i=1}^2 A_i \exp[-(t/T_1^{[i]})^{\beta_i}]. \quad (2)$$

The asymmetry A_i of each signal was held fixed at all the temperatures to avoid tradeoff effects. The fast relaxing signal was found to have only about a half of the asymmetry of the slowly relaxing signal. It is possible that these two signals are due to two different sets of muon sites giving the two frequencies observed in Fe-JST. The ratio of the two asymmetries, however, is different between Fe- and Cr-JST. Figure 4 shows the temperature dependence of the relaxation rate $1/T_1$ and the power β obtained for the two signals. We also attach the results of the magnetic susceptibility obtained using a superconducting quantum interference device (SQUID) magnetometer, which shows a departure of the field-cooling (FC) and zero-field-cooling (ZF) measurements below $T_g \sim 2$ K.

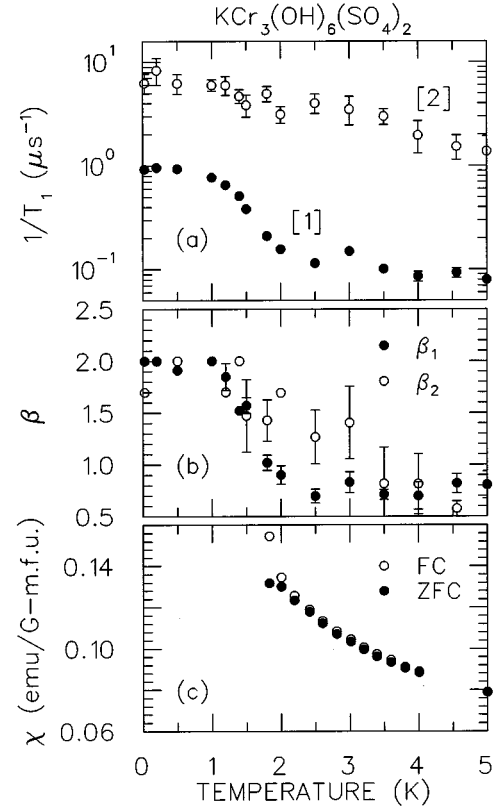


FIG. 4. The temperature dependence of (a) the relaxation rate $1/T_1^{[i]}$ and (b) the power β_i as obtained by fitting the observed results in $\text{KCr}_3(\text{OH})_6(\text{SO}_4)_2$ to Eq. (2). (c) shows the magnetic susceptibility measured by a SQUID magnetometer in field-cooling (FC) and zero-field-cooling (ZFC) procedures.

For the dominant slow-relaxing signal, we find an increase of $1/T_1$ with decreasing temperature near the history dependence temperature T_g , followed by a saturation at lower temperatures. The line shape changes from exponential above T_g to Gaussian below T_g , as indicated by the power β . These results, together with the weak-decoupling effect by LF at $T \rightarrow 0$, are quite similar to the μSR results observed in another *kagomé* lattice system $\text{SrCr}_x\text{Ga}_{12-x}\text{O}_{19}$,⁸ as well as in a charge-doped Haldane chain $(\text{Y,Ca})_2\text{Ba}(\text{Ni,Mg})\text{O}_5$.¹⁹ It should be noted that such a hardly decouplable Gaussian line shape cannot be expected in the traditional theory of muon spin relaxation (as briefly summarized above), which relies on the assumption of a Markovian process for the dynamic modulation. Therefore, the observed dynamic effect must reflect more complicated processes. A model to explain these features, proposed in Ref. 8, assumes that the depolarization of each muon is caused mostly during a small fraction of its residence time t ; the saturation of $1/T_1$ at $T \rightarrow 0$ was interpreted as a signature of quantum fluctuations. Other models with non-Markovian time evolution of the local fields would also explain the observed data. At the moment, however, it is difficult for us to find a model which explains both the μSR results and the Bragg peak reported in the neutron-scattering measurements of Cr-JST.¹³

The amplitude of the fast relaxing signal is small and the error bars in $1/T_1$ and β are rather large. This signal shows

variations mostly above T_g . We do not know the origin of this temperature variation. Note that this signal also shows the Gaussian shape at low temperatures — $\beta(T=25 \text{ mK}) = 1.67$ — which is hardly decoupled by applied longitudinal fields.

Although difficult to prove, it is very likely that the locations of the muon sites in the unit cell are the same for Fe- and Cr-JST. If this is the case, the results of Fe-JST exclude the possibility that the local field for the $q=0$ structure may cancel due to the symmetry of moments with respect to the muon site. Then the dynamic effects observed at low temperatures reflect intrinsic processes rather than an accidental effect related to the symmetry of muon sites.

The clear contrast of the present results in Fe- and Cr-JST demonstrates that the ground state in Cr-JST is certainly quite different from the long-range-ordered state in Fe-JST. We can consider several possible explanations for why these two systems behave differently: (a) Fe has $S=5/2$ whereas Cr has $S=3/2$. So, the Cr-JST may involve a stronger effect of quantum fluctuations. (b) The strength of the interlayer coupling for these two systems could be different. Indeed, the slow temperature variation of the staggered magnetiza-

tion found in Fe-JST may indicate a strong three-dimensional character of spin excitations. (c) It is also possible that these two systems have different ratios/signs of the first- and second-neighbor interactions, as suggested in Ref. 12.

In conclusion, we found a strong dynamic spin fluctuation remaining in Cr-JST even at $T = 25 \text{ mK}$, far below $T_g \sim 2 \text{ K}$. This dynamic behavior manifests in an unexpected slow decoupling of the muon polarization with increasing external longitudinal fields. The clear contrast between our results in Fe- and Cr-JST indicate that the ground state of Cr-JST is quite different from the $q=0$ long-range-ordered state identified in Fe-JST. However, further experimental/theoretical studies are required to establish details of the observed dynamic ground state in Cr-JST.

We would like to acknowledge J. E. Dutrizac for instruction in the synthesis of Cr-JST; M. Mekata, M. Collins, and P. Coleman for useful discussions; and the Packard Foundation, Mitsubishi Foundation, the Yamada Science Foundation, NSF (DMR-9510454), NSERC (Canada), and NEDO (Japan) for financial support.

*Present address: Universite Paris-Sud, Laboratoire de Physique des Solides, 91405 Orsay Cédex, France.

†Present Address: Los Alamos National Laboratory Los Alamos, NM 87545.

¹A. P. Ramirez, G. P. Espinosa, and A. S. Cooper, *Phys. Rev. B* **45**, 2505 (1992).

²C. Broholm *et al.*, *Phys. Rev. Lett.* **65**, 3173 (1990).

³J. von Delft and C. L. Henley, *Phys. Rev. B* **48**, 965 (1993); P. W. Leung and V. Elser, *ibid.* **47**, 5459 (1993); E. F. Shender and P. C. W. Holdsworth, *Fluctuations and Order: The New Synthesis* (Springer-Verlag, Berlin, 1994).

⁴Jan N. Reimers and A. J. Berlinsky, *Phys. Rev. B* **48**, 9539 (1993).

⁵I. Syôzi, *Prog. Theor. Phys.* **VI**, 306 (1951); K. Kanô and S. Naya, *ibid.* **10**, 158 (1953).

⁶A. B. Harris, C. Kallin, and A. J. Berlinsky, *Phys. Rev. B* **45**, 2899 (1992); A. Keren, *Phys. Rev. Lett.* **72**, 3254 (1994).

⁷B. Martínez *et al.*, *Phys. Rev. B* **46**, 10 786 (1992).

⁸Y. J. Uemura *et al.*, *Phys. Rev. Lett.* **73**, 3306 (1994).

⁹X. Obradors *et al.*, *Solid State Commun.* **5**, 189 (1988).

¹⁰R. Wang, W. F. Bradley, and H. Steinfink, *Acta Crystallogr.* **18**, 249 (1965).

¹¹M. Takano, T. Shinjo, and T. Takada, *J. Phys. Soc. Jpn.* **30**, 1049 (1971).

¹²M. G. Townsend, G. Longworth, and E. Roudaut, *Phys. Rev. B* **33**, 4919 (1986).

¹³C. Broholm *et al.* (unpublished); A.P. Ramirez *et al.*, *J. Appl. Phys.* **73**, 5658 (1993).

¹⁴J. E. Dutrizac and S. Kaiman, *Can. Mineral.* **50**, 151 (1976).

¹⁵A. Schenck, *Muon Spin Rotation Spectroscopy: Principles and Application in Solid State Physics* (Hilger, Bristol, 1986).

¹⁶R. S. Hayano *et al.*, *Phys. Rev. B* **20**, 850 (1979).

¹⁷Y. J. Uemura *et al.*, *Phys. Rev. B* **31**, 546 (1985).

¹⁸A. Keren, *Phys. Rev. B* **50**, 10 039 (1994).

¹⁹K. Kojima *et al.*, *Phys. Rev. Lett.* **74**, 3471 (1995).